Resistance and susceptibility QTL identified in a rice MAGIC population by screening with a minor-effect virulence factor from *Xanthomonas oryzae* pv. *oryzae*

Alejandra I. Huerta[1,†,a] (iD), Emily E. Delorean[1,‡,b], Ana M. Bossa-Castro[1] (iD), Bradley W. Tonnessen[1,c], Chitra Raghavan[2,d], Rene Corral[1] (iD), Álvaro L. Pérez-Quintero[1] (iD), Hei Leung[2], Valérie Verdier[3] (iD) and Jan E. Leach[1,*] (iD)

[1]*Department of Agricultural Biology, Colorado State University, Fort Collins, CO, USA*

[2]*Division Genetics and Biotechnology, International Rice Research Institute, Manila, Philippines*

[3]*IRD, Cirad, IPME, Univ Montpellier, Montpellier, France*

Summary

Effective and durable disease resistance for bacterial blight (BB) of rice is a continuous challenge due to the evolution and adaptation of the pathogen, *Xanthomonas oryzae* pv. *oryzae* (*Xoo*), on cultivated rice varieties. Fundamental to this pathogens' virulence is transcription activator-like (TAL) effectors that activate transcription of host genes and contribute differently to pathogen virulence, fitness or both. Host plant resistance is predicted to be more durable if directed at strategic virulence factors that impact both pathogen virulence and fitness. We characterized Tal7b, a minor-effect virulence factor that contributes incrementally to pathogen virulence in rice, is a fitness factor to the pathogen and is widely present in geographically diverse strains of *Xoo*. To identify sources of resistance to this conserved effector, we used a highly virulent strain carrying a plasmid borne copy of Tal7b to screen an indica multi-parent advanced generation inter-cross (MAGIC) population. Of 18 QTL revealed by genome-wide association studies and interval mapping analysis, six were specific to Tal7b (q*BB-tal7b*). Overall, 150 predicted Tal7b gene targets overlapped with q*BB-tal7b* QTL. Of these, 21 showed polymorphisms in the predicted effector binding element (EBE) site and 23 lost the EBE sequence altogether. Inoculation and bioinformatics studies suggest that the Tal7b target in one of the Tal7b-specific QTL, q*BB-tal7b*-8, is a disease susceptibility gene and that the resistance mechanism for this locus may be through loss of susceptibility. Our work demonstrates that minor-effect virulence factors significantly contribute to disease and provide a potential new approach to identify effective disease resistance.

Introduction

The most significant bacterial disease impacting rice is bacterial blight (BB), caused by *Xanthomonas oryzae* pv. *oryzae (Xoo)*. In the field, BB severity depends on host genotype, pathogen pressure and environmental conditions. An optimal agronomic practice to manage BB is the deployment of resistant varieties. Historically, available resistance to manage the disease has relied on major resistance (*R*) genes that detect bacterial virulence effectors. Unfortunately, the efficacy of *R*-genes is frequently lost over time due to the pathogen's adaptation to a genotype and the evolution of new pathogenic races (Mew *et al*., 1992; Quibod *et al*., 2016). Identifying new sources of resistance that are effective and durable for BB is a pressing challenge for rice production, considering the increasing demand for the grain.

Collectively, effectors dictate bacterial virulence and pathogenicity, and some provide a selective advantage to the pathogen, that is, their loss negatively impacts bacterial fitness (Leach *et al*., 2001; Ponciano *et al*., 2003). One strain or pathogen population may carry multiple effectors with redundant function, and some populations can house highly variable effector repertoires (Quibod *et al*., 2016; Vera Cruz *et al*., 2000). Furthermore, some effectors have a large effect on pathogen virulence (major effects) and can mask the role of minor-effect virulence factors, effector proteins that have moderate yet significant effects on the host (Bai *et al*., 2000). Knowing the contribution of both major- and minor-effect factors to pathogen fitness and virulence as well as their gene targets can guide breeding strategies towards stabilizing disease resistance (Leach *et al*., 2001).

Important to *Xoo* virulence are transcription activator-like (TAL) effectors, which induce expression of plant host genes (Boch *et al*., 2014; Hutin *et al*., 2015; Römer *et al*., 2010; Yang *et al*., 2000). Gene induction is dependent on the repeat variable diresidues (RVDs) in the central repeat region (CRR) of the protein. TAL effector RVD's bind to specific sequences, the effector

binding element (EBE), located in the promoters of target plant genes (Boch *et al.*, 2009; Moscou and Bogdanove, 2009). Frequently, TAL effectors target susceptibility (*S*) genes in the host genome, enhancing disease severity (Perez-Quintero and Szurek, 2019; Streubel *et al.*, 2013). To avoid pathogen infection, plants have evolved TAL effector-associated resistance [for a review, see (Hutin *et al.*, 2015)]. Included in the latter are dominant TAL effector-dependent resistance mechanisms (Zhang *et al.*, 2015), dominant non-transcriptional dependent (Schornack *et al.*, 2004; Triplett *et al.*, 2016) and resistance through loss of susceptibility (Hutin *et al.*, 2015). The last example includes both natural variation in susceptibility alleles, like *Xa5/xa5* (Iyer and McCouch, 2004) and those generated through genome editing technologies where the EBEs of *S*-genes are edited resulting in resistance (Boch *et al.*, 2014; Oliva *et al.*, 2019).

In a recent comparative genomic study, a total of 181 TAL effectors were identified from ten Philippine *Xoo* isolates that represented the ten different Philippine races (Quibod *et al.*, 2016). Based on RVD compositions, these effectors were classified into 30 TAL effector families (TEF). The TAL effectors within a family have similar RVD sequences, suggesting functional similarities and shared host gene targets. However, function has only been characterized for nine of the 30 TEF, based on one or two representative major-effect TAL effectors for each family. One TEF containing nine homologues that remains to be characterized is TEF7 (Quibod *et al.*, 2016). Within this family, one member, Tal7b, plays an incremental, but significant role in bacterial virulence and fitness (Bai *et al.*, 2000). Each *Xoo* strain may have nine or more TAL effectors, with only one or two per strain in the major-effect virulence factor category. Thus, the diversity among the families and the conservation of minor-effect TAL effectors, such as Tal7b, among geographically distinct strains raises the questions '*why are TAL effectors with minor-effects conserved?*' and '*what are their host targets?*'

Assuming *R*-gene durability is linked to the relative importance of effectors to pathogen virulence, one potential strategy to select for long-lasting resistance in the field is to screen for sources of resistance that target bacterial fitness factors, including highly conserved minor-effect virulence effectors such as Tal7b (Leach *et al.*, 2001; Vera Cruz *et al.*, 2000). To this end, we used a two-pronged approach aimed at identifying new sources of resistance that target this specific TAL effector. We used a multi-parent advanced generation inter-cross (MAGIC) population generated from eight elite founders from the indica subgroup of rice (Bandillo *et al.*, 2013; Raghavan *et al.*, 2017). This powerful resource captures the genetic diversity of multiple founders that have been recombined over several generations to create a population with large phenotypic diversity ideal for high-resolution trait mapping (Bandillo *et al.*, 2013; Raghavan *et al.*, 2017). In addition, we

exploited the functionally and bioinformatically deciphered TAL effector code to predict gene targets for Tal7b within the QTL (Boch *et al.*, 2009; Moscou and Bogdanove, 2009) and to gain insights into the mechanisms for Tal7b resistance and susceptibility.

Here, we report the identification of 18 BB disease resistance QTL, 12 of which target BB strain PX099[A], and six of which are unique to PXO99[A] overexpressing *tal7b*. We identified 150 putative Tal7b EBEs within these loci and show that several of the resistance QTL harbour polymorphisms in or near the predicted Tal7b EBE. Our results suggest that Tal7b contributes to *Xoo* virulence by targeting multiple novel *S*-genes in rice. Altogether, our data broadens the perspective on effector-triggered susceptibility to emphasize that one effector may target multiple *S*-genes, that is quantitative susceptibility, and suggests that quantitative resistance can result from inactivation of one or more *S*-genes.
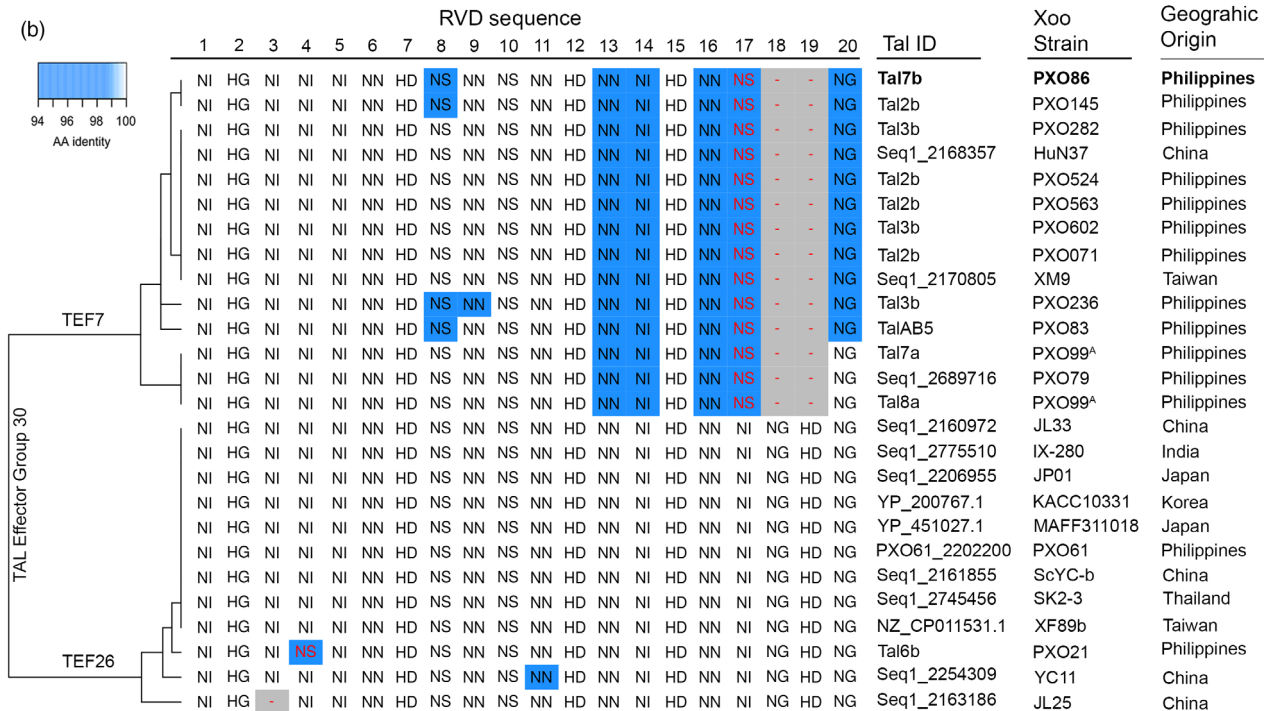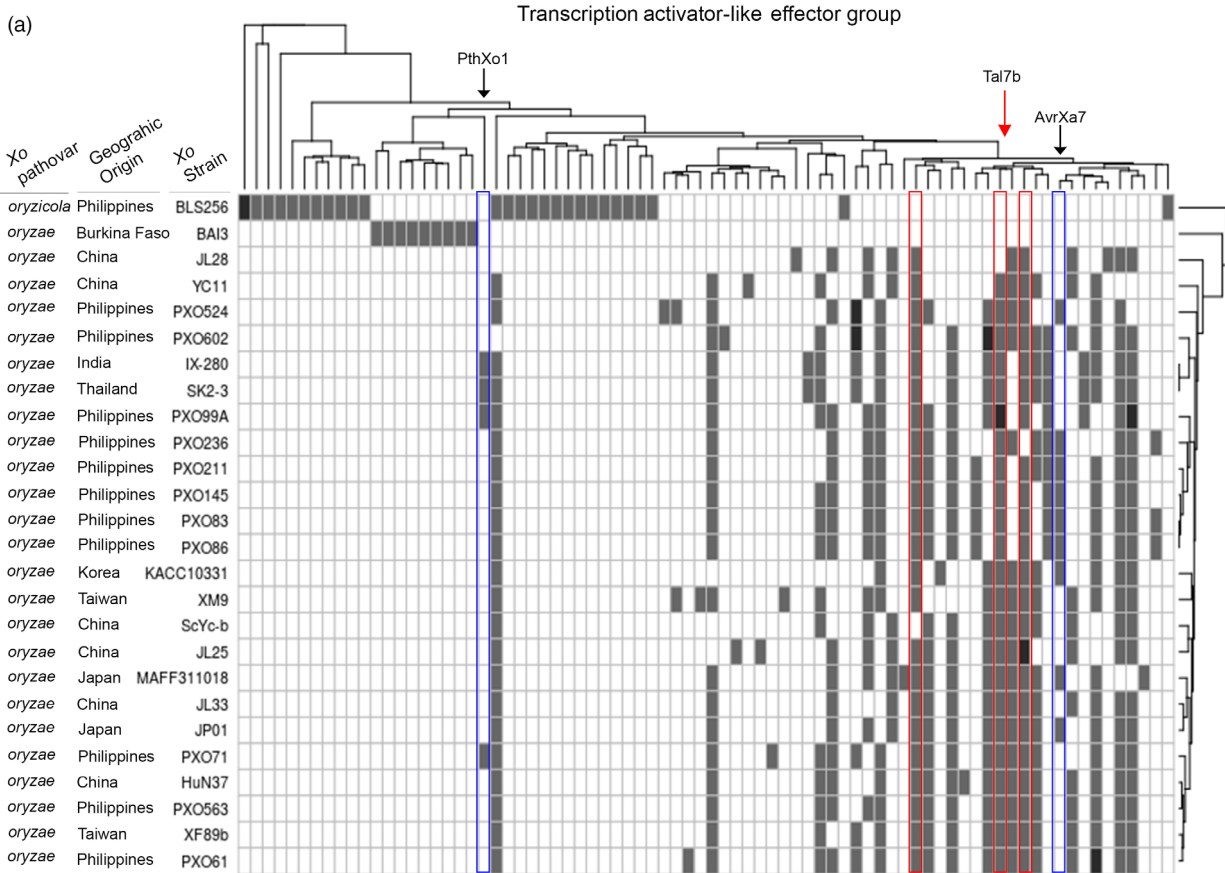
Results and discussion

Tal7b is a conserved TAL effector in Asian *X. oryzae* pv. *oryzae* strains

Tal7b is one of nine TAL effectors in the uncharacterized TAL effector family 7 (Quibod *et al.*, 2016). Originally named ab4.5, Tal7b incrementally contributes to pathogen virulence (Bai *et al.*, 2000), and thus, was selected as a minor-effect virulence factor to screen for resistance sources. The effector gene was cloned from *Xoo* strain PXO86. Sequence analysis confirmed the cloning of *tal7b* and showed that the CRR of *tal7b* is composed of 18 repeats and has RVD sequence: NI HG NI NI NI NN HD NS NN NS NN HD NN NI HD NN NS NG (Figure 1 and Booher *et al.*, 2015).

All complete genomes of *X. oryzae* were queried for TAL effectors, and their RVD sequences were extracted and classified into TAL effector groups using DisTAL (Hutin *et al.*, 2015; Pérez-Quintero *et al.*, 2015). This analysis showed Tal7b homologues are present in all complete genomes of Asian *Xoo* strains except in strain JL28 and were absent in all sequenced *Xoo* strains of African origin (Figure 1). Tal7b was not detected in *X. o.* pv. *oryzicola* (*Xoc*), the causal agent of bacterial leaf streak of rice. At least one copy of the effector was found in representatives of the ten different *Xoo* races (Figure 1a). A Tal7b variant with two additional repeats in the CRR was also found in several Asian *Xoo* strains (Figure 1b). These variants were originally grouped into a separate TAL effector family, TEF26 (Quibod *et al.*, 2016), and are 93% identical to Tal7b at the amino acid level (Figure S1). Although they varied at the DNA level, sequence alignment of Tal7b homologues from all strains indicates 100% similarity in RVD composition and sequence, except from those with the two extra repeats (Figure 1b). Both TEF7 and TEF26, which include Tal7b, are now classified into one *Xoo* TAL effector group (Group 30) according to the DisTAL tree (Figure 1; Lang

Figure 1 Tal7b is conserved among *Xanthomonas oryzae* pv. *oryzae* (*Xoo*) strains of Asian origin. (a) TAL effector profiles from 24 Asian strains of *Xoo* and one representative strain of African *Xoo* (BAI3), and an Asian *X. o.* pv. *oryzicola* (*Xoc*) strain (BLS256) were classified into groups according to DisTAL tree (Pérez-Quintero *et al.*, 2015). TAL groups are listed in order from left to right and conserved TAL effector groups are outlined in red; major TAL effector groups containing PthXo1 and AvrXa7 are boxed in blue; grey/white shading indicates the presence or absence of TAL effector in a strain; black represents multiple copies of that TAL effector or a homologue in that strain. The tree at the top shows the phylogenetic distances between TAL effector groups, and the parsimony tree on the right is based on whole genome sequences. (b) Variation and phylogenetic relationships of Tal7b homologues in Asian strains of *Xoo* are shown for each TAL effector along with their RVD sequence, TAL ID, strain name and specific geographic origin. The heatmap indicates nucleotide identity for each repeat, where blue represents sequence mismatch as indicated in identity key (top left) and white shading represents 100% match among sequences. Red letters indicate the two RVD where TAL effector family (TEF) 7 and 26 members differ and missing repeats are represented as dashed red lines inside grey boxes.

(a) Transcription activator-like effector group

(b)

et al., 2019; Pérez-Quintero *et al.*, 2015). TAL effector groups 23, 30 and 32 are among the most conserved TAL effectors in *Xoo* genomes (Figure 1A). These results show that Tal7b is among the most conserved TAL effectors in Asian *Xoo* strains and are consistent with the evolutionary selection for the function of this effector in bacterial fitness.

Tal7b is a minor virulence factor, and its phenotype in interactions with rice is masked by more dominant effector activity (Bai *et al.*, 2000), in the case of PXO99[A] by PthXo1 (Yang and White, 2004). Thus, to amplify resistance and susceptibility phenotypes in our large-scale screening experiments, we created a *Xoo* PXO99[A] strain that overexpresses Tal7b. PXO99[A] also harbours two Tal7b gene homologues, *tal7a* and *tal8a*, that encode proteins 99.6% identical to the amino acid sequence of PXO86 Tal7b and show no variation in RVD sequence (Figure 1b). We cloned *tal7b* from PXO86 into the low-copy vector pHMI to create pHMI::*tal7b* and introduced the clone and empty vector control (pHMI::EV) into PXO99[A] to create PXO99[A] pHMI::*tal7b* and PXO99[A] pHMI::EV, respectively. We confirmed low expression of Tal7b in the PXO99[A] wild-type strain and demonstrated

moderate overexpression in the PXO99[A] pHMI::*tal7b* strains (Figure S2). In the following plant screening experiments, the overexpressing strain PXO99[A] pHMI::*tal7b* and the empty vector control (PXO99[A] pHMI::EV) were used for inoculations.

The indica MAGIC population segregates for resistance to PXO99[A] pHMI::EV and PXO99[A] pHMI::*tal7b*

We took advantage of the high allelic variation in the indica MAGIC population to identify resistance loci for Tal7b (Bandillo *et al.*, 2013; Raghavan *et al.*, 2017). We screened all eight founders alongside 330 F$_{6-8}$ (6th-8th generation of selfing) advanced intercrossed lines, named Advanced Inbred Lines (AILs), for resistance to PXO99[A] pHMI::EV or PXO99[A] pHMI::*tal7b*. On average, more disease (longer lesion lengths, Tukey adjusted *P*-value < 0.0001) was observed on AILs challenged with PXO99[A] pHMI::*tal7b* compared to those inoculated with PXO99[A] pHMI::EV indicating potential *S*-gene targets to Tal7b in the MAGIC population (Figure 2a, b; Tables S1 and S2). When pHMI::*tal7b* was overexpressed in PXO99[A], the overall average lesion length (17.1 cm) was 3.3 cm longer than that for PXO99[A] pHMI::EV (13.8 cm)

A. Fedearroz 50   C. IR4630-22-2-5-1-3   E. PSBRc82   G. Sanhuangzhan-2
B. IR45427-2B-2-2B-1-1   D. IR77298-14-1-2-10   F. PSBRc158   H. Sambha Mahsuri + Sub1
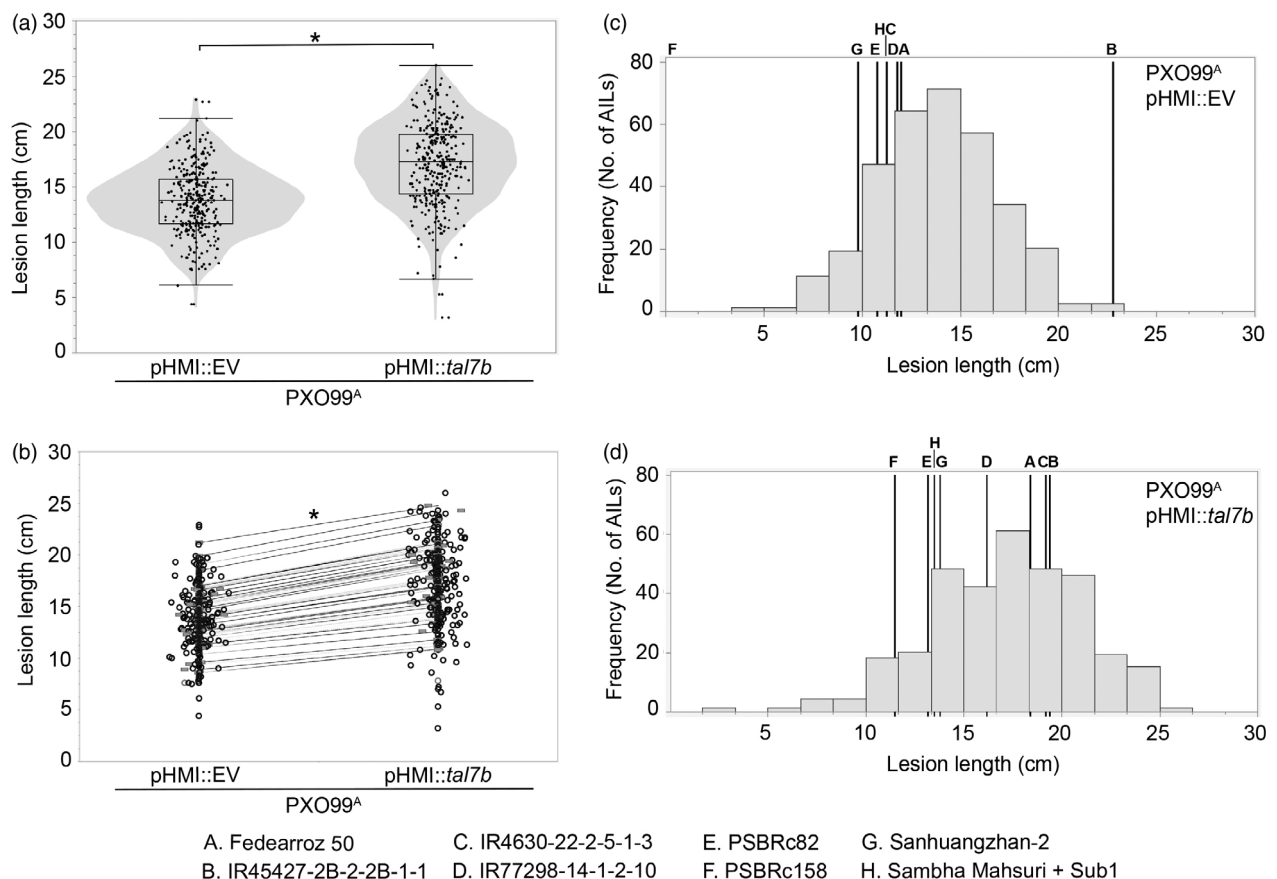
Figure 2 Distribution of the phenotypic response (lesion length in cm) of MAGIC AILs to strain PXO99[A] with *tal7b* (pHMI::*tal7b*) or the empty vector control (pHMI::EV). (a) Violin plots represent the distribution of the least square means (LS-Means) of bacterial blight disease lesion lengths on 330 MAGIC AILs and the eight founders inoculated with PXO99[A] pHMI::EV (left) or pHMI::*tal7b* (right). Embedded box and whisker plots represent 50% of the values around the median (bold). The asterisk (*) represents Tukey adjusted *P*-value < 0.001. (b) Each point on the scatter plot represents the LS-Means of lesion length for each of the 330 AIL screened. The black lines connecting each point highlight the 63 AIL with significantly longer lesion lengths in response to PXO99[A] pHMI::EV (left) compared to PXO99[A] pHMI::*tal7b* (right) (Tukey adjusted *P*-value < 0.05). Histograms represent the frequency distribution of the lesion length (LS-Means) in the MAGIC AILs after inoculation with (c) PXO99[A] pHMI::EV and (d) PXO99[A] pHMI::*tal7b*. Histograms are overlaid on LS-Means of the lesion lengths for the eight founder parents of the indica MAGIC population. PSBRc82 (F) was not included in the PXO99[A] pHMI::EV screen in panel c because of poor germination.

(Table S1). These data confirm that Tal7b is a minor-effect virulence factor that contributes incrementally to *Xoo* virulence.

None of the eight MAGIC founders displayed a strong qualitative resistance phenotype (LL < 5 cm) to either strain tested (Figure 2c, d; Table S3). Of the 330 AILs screened, 24 and 32 showed shorter lesion lengths to PXO99[A] pHMI::EV and PXO99[A] pHMI::*tal7b* than the most resistant parent for each treatment, Samba Mahsuri + *Sub1* (LL = 9.8 cm) and PSBRc158 (LL = 11.5 cm), respectively (Figure 2c, d; Table S3). At the opposite extreme, one and 96 of the 330 AIL were more susceptible than the most susceptible parent, IR4527-2B-2-2B-1-1, to PXO99[A] pHMI::EV (LL = 22.8) and PXO99[A] pHMI::*tal7b* (LL = 19.4), respectively (Figure 2c, d; Table S3). The normal distribution and continuous variation observed in the phenotypic response of AIL screened to PXO99[A] pHMI::EV and PXO99[A] pHMI::*tal7b*, in conjunction with the transgressive segregation observed for both strains, indicate that the MAGIC population segregates for resistance and susceptibility to these strains (Figure 2c,d). Moreover, the lack of large reductions or increases in resistance or susceptibility suggests that these traits are controlled by multiple small and moderate effect resistance and susceptibility loci.

Marker-assisted analyses identify loci associated with resistance to *Xoo* PXO99[A] pHMI::EV and PXO99[A] pHMI::*tal7b*

Interval mapping (IM) and genome-wide association studies (GWAS) were used to map resistance loci for PXO99[A] pHMI::*tal7b* (Tal7b). IM analyses identified a total of 18 QTL associated with disease resistance to both PXO99[A] pHMI::EV and PXO99[A] pHMI::*tal7b* (Figure S3; Tables S4, S5). Nine QTL, named qBB-PXO99[A], were detected in response to PXO99[A] pHMI::EV on chromosomes 1, 5, 7, 8, 10, 11 and 12 (Figure S3a; Table S4). Similarly, nine QTL were identified to PXO99[A] pHMI::*tal7b* and named qBB-*tal7b* on chromosomes 1, 3, 5, 8, 10, 11 and 12 (Figure S3b; Table S5). Of the 18 QTL detected, only the QTL on chromosomes 5 (qBB-PXO99[A]-5 and qBB-*tal7b*-5) and 10 (qBB-PXO99[A]-10-1 and qBB-*tal7b*-10-1, qBB-PXO99[A]-10-2 and qBB-*tal7b*-10-2) were common to both strains and thus were not unique to Tal7b (Figure S3; Tables S4, S5).

The QTL on chromosome 5, qBB-PXO99[A]-5 and qBB-*tal7b*-5, explained 15.7% and 12.6% of the phenotypic variance observed, respectively, and were supported by strong SNP associations in GWAS (Tables S4-S7). Of the 43 significantly associated SNP markers genome-wide, 33 clustered on chromosome 5 (Figure 3; Table S6) and four of these were within the 95% confidence interval of qBB-PXO99[A]-5 (Table S4, S6). This QTL was previously detected in the indica MAGIC population in screenings for bacterial blight QTL (Bossa-Castro *et al.*, 2018). The QTL and its associated SNP markers overlapped with the mapped bacterial blight susceptibility/resistance gene *Xa5/xa5*, a broad-spectrum disease resistance gene that functions independently of TAL effector binding specificity through the naturally occurring recessive allele (*xa5*) of the basal transcription factor TFIIA©5 (*Xa5*) (Figures 3, 4a; Blair *et al.*, 2003; Huang *et al.*, 2016; Iyer and McCouch, 2004).

The remaining ten significant markers identified by GWAS for PXO99[A] pHMI::EV were associated with previously identified QTL for BB on chromosome 11 (qBBR11) (Chen *et al.*, 2012), but did not map to qBB-PXO99[A]-11, the QTL identified by IM in this study (Figures 3, 4a, Figure S2). The QTL identified on chromosomes 5 and 11, both supported by IM and GWAS, confirm that our approach provides robust data to detect previous and novel QTL conferring resistance to one minor-effect virulence factor and also refine previously identified QTL, as in the case for qBB-*tal7b*-11, qBB-*tal7b*-12-1, qBB-PXO99[A]-12-1 and qBB-PXO99[A]-12-2 (Figure 4a, Figure S8).

Unique resistance QTL to minor-effect virulence factor Tal7b

For PXO99[A] pHMI::*tal7b*, a total of 29 significantly associated SNP markers were identified by GWAS (MLM analysis, *P*-value < 0.001) on chromosomes 5, 8, 11 and 12 (Figure 3b, Table S7). Twenty of the 29 associated SNP markers for PXO99[A] pHMI::*tal7b* clustered on chromosome 5, six of which overlapped with the QTL identified through IM on the same chromosome for PXO99[A] pHMI::Tal7b (qBB-*tal7b*-5) and PXO99[A] pHMI::EV (qBB-PXO99[A]-5) (Figure 3, 4a; Tables S5, S7 and S8). All 20 SNP markers associated with PXO99[A] pHMI::*tal7b* on chromosome 5 were also associated with PXO99[A] pHMI::EV (Tables S6, S7). The remaining nine SNP markers were distributed into two smaller clusters and were unique to PXO99[A] overexpressing Tal7b (pHMI::*tal7b*). Four SNP markers overlapped with qBB-*tal7*-8, the 705 kb resistance QTL to PXO99[A] pHMI::*tal7b* on chromosome 8 (Figure 3b, 3d). Four different SNP markers converged on qBB-*tal7b*-12-2, the 236 Kb QTL on chromosome 12, which also overlapped with the previously described QTL for disease resistance to BB, G-BB-AQBT0219 (Figures 3, 4a; Tables S6, S8) (Tello-Ruiz *et al.*, 2017).

The final marker associated with PXO99[A] pHMI::*tal7b* on chromosome 11, S11_28697250, did not overlap with any of the QTL identified by IM on this chromosome in this study, qBB-PXO99[A]-11 and qBB-tal7b-11 (Tables S4-S7). S11_28697250 did overlap with three previously reported QTL including AQAQ017 (Tello-Ruiz *et al.*, 2017) and RL-RB-qRBr-11.2 (Ashkani *et al.*, 2013), both of which are associated with rice blast disease resistance, and qBBR11, conferring BB disease resistance (Figures 4a, Figure S8) (Chen *et al.*, 2012). Overall, we identified six resistance QTL to PXO99[A] pHMI::*tal7b*, demonstrating the genetic resolution housed in the MAGIC population was sufficient to identify novel QTL for a minor-effect TAL effector.

Tal7b gene targets converge on QTL identified for PXO99[A] pHMI::*tal7b*

The deciphered TAL effector code allows for the computational prediction of Tal7b gene targets in the rice genome (Boch *et al.*, 2009; Moscou and Bogdanove, 2009). To explore if putative Tal7b gene targets converged on identified QTL in this study, we used two tools, TALE-NT 2.0 (Doyle *et al.*, 2012) and Talvez (Pérez-Quintero *et al.*, 2013), to predict Tal7b targets in the rice genome (Figure 4b, c). A total of 97,219 genome-wide EBEs were predicted for Tal7b (Figure 4e). Next, the predicted EBEs and their positions were aligned with the physical positions of the significantly associated SNP markers and QTL identified in this study. This analysis revealed 153 EBE in 148 different gene candidates that were (i) predicted Tal7b rice gene targets and (ii) in or near one of the QTL identified in this study (Figure 4d; Table S9). Of the 153 EBE, 126 or 80% converged on qBB-*tal7b*-1, qBB-*tal7b*-3 and the two qBB-*tal7b* QTL on chromosome 10 (Figure 4b). The remaining 27 EBEs overlapped with Tal7b unique QTL on chromosome 5, 8, 11 and 12 (Figure 4b; Table S9). Among the top 10, Tal7b gene targets in these QTL are a zinc finger (LOC_Os03g05480), a ribosomal protein (LOC_Os01g14830) and several hypothetical proteins
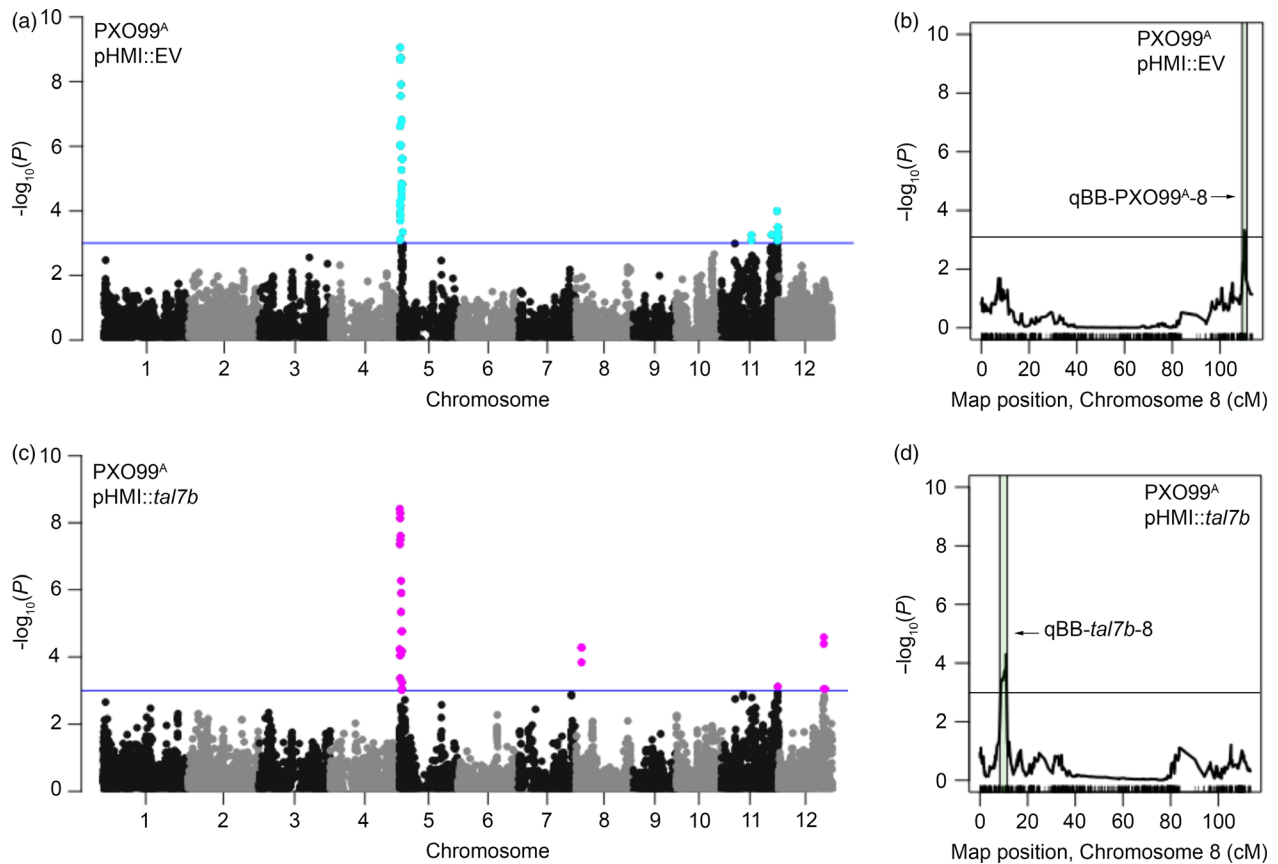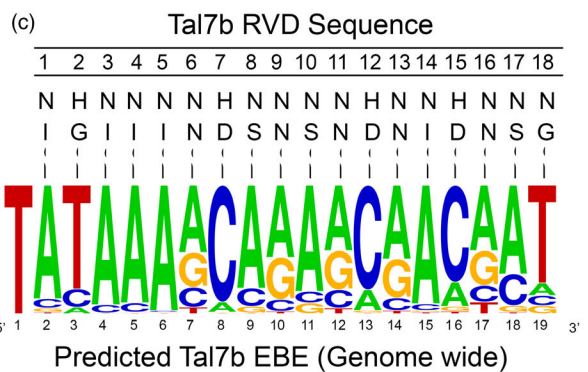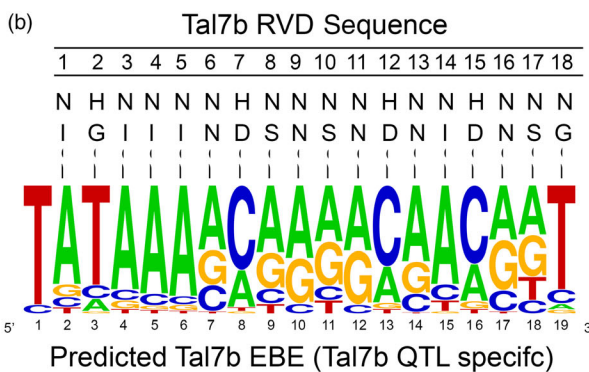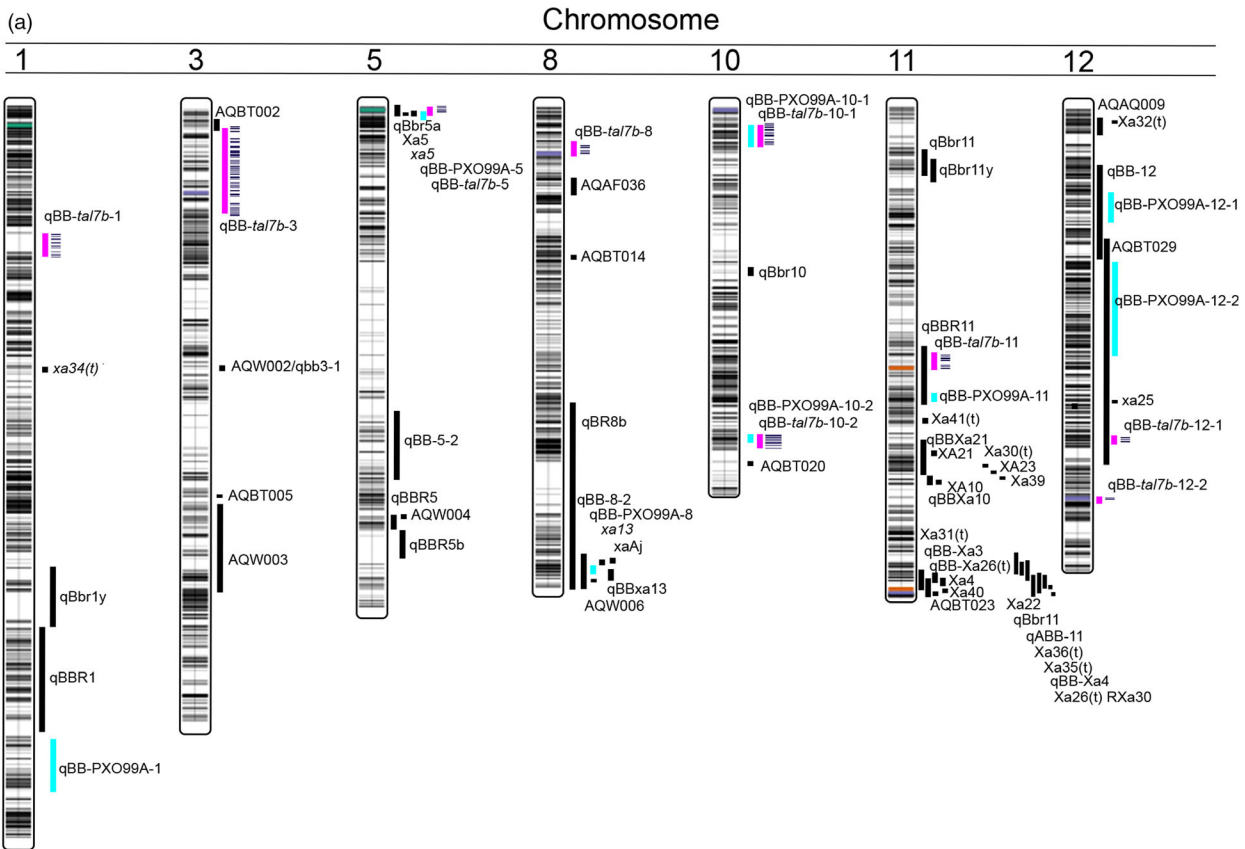
Figure 3 Detection of QTL conferring resistance to PXO99[A] carrying pHMI::EV or pHMI::*tal7b*. Manhattan plots and simple interval mapping show the genomic location on the x-axis and the negative logarithm of the *P*-values on the y-axis. Solid blue line indicates a significance threshold of $P \leq 0.001$. (a, b) GWAS results show significant associations to (a) PXO99[A] pHMI::EV on chromosomes 5 and 11 (cyan; Table S7) and (b) PXO99[A] pHMI::*tal7b* on chromosomes 5, 8, 11 and 12 (magenta; Table S8). (c, d) Simple interval mapping featuring unique QTL to Tal7b on chromosome 8, qBB-PXO99[A]-8 and qBB-*tal7b*-8. Shaded regions indicate 1-LOD supporting intervals for (c) qBB-PXO99[A]-8 to PXO99[A] pHMI::EV, which is distinct from the peak for (d) qBB-*tal7b*-8 to PXO99[A] pHMI::*tal7b*.

(LOC_Os08g04900, LOC_Os08g04910, LOC_Os03g11874) (Figure 4e; Table S9). Two of the top 10 gene targets with Tal7b EBEs, LOC_Os01g14100 and LOC_Os03g83340, were significantly induced (>2 Log$_2$ Fold Change) in a susceptible rice variety when challenged with PXO99[A] (Pérez-Quintero *et al.*, 2018) and one, LOC_Os01g135770, was significantly down-regulated (Pérez-Quintero *et al.*, 2018). Additional genome-wide putative targets include homologues of the nodulin MtN3 family proteins that encode *SWEET* sucrose transporter genes, which have been reported as major TAL effector susceptibility gene targets in rice, citrus and cotton (Cohn *et al.*, 2014; Cox *et al.*, 2017; Yang *et al.*, 2006). However, the putative Tal7b *OsSWEET* gene targets are not located within the Tal7b unique QTL identified in this study (Figure 4a; Table S8). Other targets near the identified QTL included a putative brassinosteroid insensitive 1-associated receptor kinase 1 precursor (*OsSerk1/OsBAK1*, LOC_Os08g07760), a putative dehydrin (DHN, LOC_Os11g26790), a calmodulin-binding protein (Ca M-binding protein, LOC_Os12g36920) and a spotted leaf 11 gene (SPL11, LOC_Os12g38210) (Figure 4a; Table S8).

Next, using data from the 3K rice genome project (Wang *et al.*, 2018), we aligned and analysed the promoters of the putative Tal7b rice gene targets in each of the eight indica MAGIC founders. We focused on the targets that are unique to PXO99[A] pHMI::*tal7b*, and thus, excluded targets in QTL qBB*tal7b*-5, qBB*tal7b*-10-1 and qBB*tal7b*-10-2 (Figure 4a). Of the remaining 119 Tal7b putative gene targets, we identified in at least one of the eight MAGIC founders: 23 EBEs with polymorphic sites in the EBE sequence (Figure 5a; Table S9); 54 with downstream or upstream shifts surrounding the EBE sequence (Figure 5b;

Figure 4 Predicted Tal7b gene targets overlap with QTL conferring resistance to PXO99[A] pHMI::*tal7b*. (a) Integrated physical map of rice chromosomes 1, 3, 5, 8, 10, 11 and 12 showing QTL identified in this study for PXO99[A] pHMI::EV (cyan), PXO99[A] pHMI::*tal7b* (magenta), predicted Tal7b targets (horizontal lines) and previously described resistance loci for bacterial blight (vertical lines). Detailed physical location for mapped loci is listed in Table S8. (b) Sequence logo showing predicted EBE of Tal7b using predicted targets in PXO99[A] pHMI::*tal7b*-specific QTL only. (c) Sequence logo showing predicted EBE of Tal7b using predicted targets from a genome-wide scan. (d) Predicted Tal7b gene targets per QTL unique for PXO99[A] pHMI::*tal7b*. (e) Top ten predicted Tal7b gene targets that overlap with PXO99[A] pHMI::*tal7b*-specific QTL.
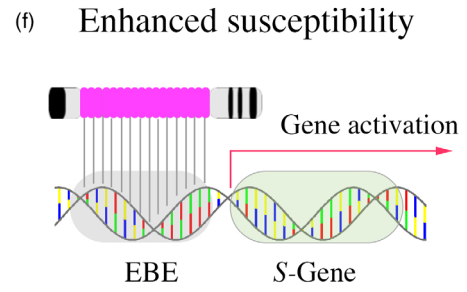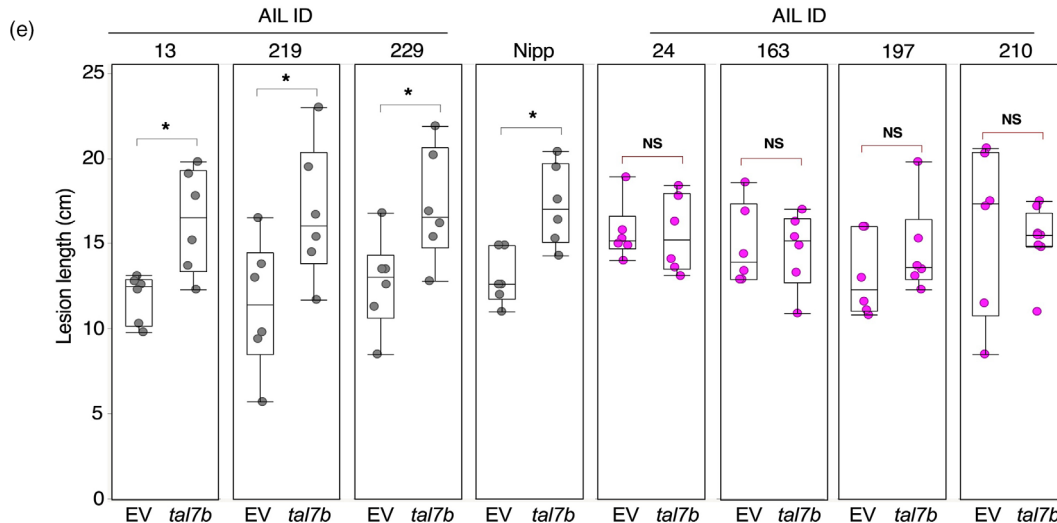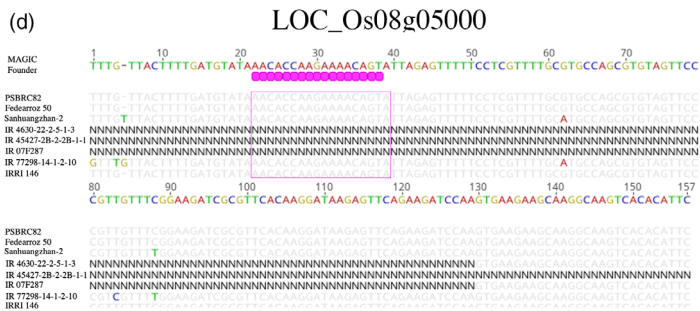
(a) Chromosome

(b) Tal7b RVD Sequence

Predicted Tal7b EBE (Tal7b QTL specifc)

(c) Tal7b RVD Sequence

Predicted Tal7b EBE (Genome wide)

(d) Predicted Tal7b targets

QTL	# of targets
qBBtal7b-1	27
qBBtal7b-3	56
qBBtal7b-5	7
qBBtal7b-8	9
qBBtal7b-10-1	27
qBBtal7b-10-2	16
qBBtal7b-11	1
qBBtal7b-12-1	4
qBBtal7b-12-2	1

(e) Top 10 Tal7b Genes Targets in QTL

Chr.	Locus	Function
3	LOC_Os03g05480	ZOS3-01 - C2H2 zinc finger
1	LOC_Os01g14830	ribosomal protein L3
8	LOC_Os08g04900	hypothetical protein
8	LOC_Os08g04910	expressed protein
1	LOC_Os01g13570	phosphoglycerate mutase
1	LOC_Os01g14100	BT1 family protein
3	LOC_Os03g08330	ZIM domain containing protein
3	LOC_Os03g11874	expressed protein
1	LOC_Os01g14260	transposon protein
5	LOC_Os05g01600	actin

Figure 5 Allelic variation in predicted Tal7b rice targets in MAGIC founders identify putative susceptibility genes for Tal7b. Tal7b predicted gene target with (a) polymorphic events in the EBE site itself; (b) downstream or upstream shifts in the promoter region between the EBE and the start codon or the region 1 kb upstream the EBE site (or both); (c) indels; and (d) complete absence of the EBE site in at least one or more of the eight f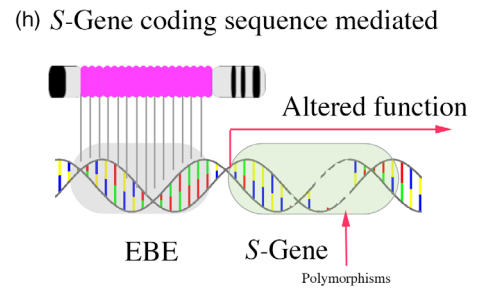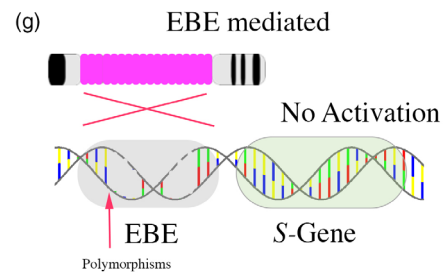ounders (Table S9). (e) Lesion lengths on AIL and Nipponbare (Nipp) inoculated with PXO99[A] pHMI::EV or PXO99[A] pHM1::*tal7b*. The AIL ID number is listed above each pairwise comparison box. Asterisks indicate significant differences between treatments, as determined by one-way ANOVA (P-value ≤ 0.05, Table S11). NS represents no significant differences between treatments. (f-h) Model proposing how resistance in q-BB*tal7b*-8 may contribute to resistance through loss of susceptibility by harbouring polymorphisms in the (g) Tal7b EBE or (h) *S*-gene coding sequence, disabling activation or function of the putative *S*-gene.

Table S9); 18 with indels in the EBE sequence (Figure 5c; Table S9); and 10 which lacked the EBE sequence in the promoter region of the putative target gene (Figure 5d; Table S9). In a survey of published transcriptome data, 21 of the 119 corresponding putative Tal7b targets were differently expressed in rice inoculated with at least one of the three *Xoo* strains harbouring Tal7b (Table S9). Overall, the polymorphisms in the EBE sequence or in the promoter region and the corresponding changes in target gene expression are reminiscent of resistance through loss of susceptibility and are consistent with a model that allelic variation at these positions may serve as a source of recessive resistance against *Xoo* strains harbouring Tal7b (Figure 5f-h).

qBB-*tal7b*-8 harbours a susceptibility allele to PXO99[A] pHMI::*tal7b*

The QTL that mapped to chromosome 8 and was unique for PXO99[A] pHMI::*tal7b,* named qBB-*tal7b*-8, was selected to further characterize the resistance mechanism governing this locus. Fourteen MAGIC AILs (AIL: 13, 24, 156, 163, 197, 210, 219, 222, 225, 229, 234, 237, 250 and 267) with resistant and susceptible marker alleles (Table S7) on chromosome 8 were selected from the 330 AILs originally screened. These lines and Nipponbare, which served as a susceptible control, were re-screened for their responses to PXO99[A] pHMI::EV and PXO99[A] pHMI::*tal7b*. A subset of these lines (13, 219, 229) and Nipponbare showed significantly longer lesions (4.7 cm, P-value < 0.001) in response to PXO99[A] pHMI::*tal7b* (average LL = 16.9 cm) than to PXO99[A] pHMI::EV (average LL = 12.2 cm) (Figure 5e; Table S11). The remaining 11 AILs that were re-screened, including lines 24, 163, 197 and 210 (Figure 5e; Table S11), did not differ in the observed lesion lengths to either bacterial strain, regardless of the presence or absence of pHMI:: *tal7b*. Among these 11 non-responsive lines, the average lesion length for PXO99[A] pHMI::*tal7b* was 13.1 cm and 12.5 cm for PXO99[A] pHMI::EV. The absence of a significant lesion length difference in the majority of lines with variant alleles in qBB-*tal7b*-8 suggests that this QTL houses a minor yet significant susceptibility allele responsive to Tal7b, and that the resistance observed may be through loss of susceptibility, as proposed in Figure 5g-h.

Conclusions

Long-lasting disease resistance is a highly sought-after trait for crop breeding programmes. However, achieving durable resistance is a challenge because pathogen populations continually evolve to overcome deployed host resistance. The pathogen population changes occur through mutation of the pathogen effector genes targeted by specific plant resistance genes, or through invasion or build-up of novel pathogen populations that do not harbour the targeted effector. Many widely studied *Xoo*

effectors are TAL effectors, including PthXo1 and AvrXa7, which are major virulence factors (Bai *et al.*, 2000; Yang and White, 2004), but these are not widely conserved in the global pathogen population (Figure 1; Lang *et al.*, 2019; Quibod *et al.*, 2016)). In contrast, a number of TAL effectors, such as Tal7b and related effectors, are individually minor contributors to pathogen virulence (Figure 2; Bai *et al.*, 2000), and their distribution is widespread in *Xoo* populations (Figure 1). We and others postulate that incorporating resistances that target these widespread effectors will help stabilize plant disease resistance, increasing its durability (Leach *et al.*, 2001; Mundt, 2014). Towards this end, we employed an innovative rice MAGIC population that contains the genetic diversity of eight indica parents (Bandillo *et al.*, 2013; Bossa-Castro *et al.*, 2018) to identify potential durable disease resistance loci that target the widespread minor virulence effector Tal7b.

Six QTL specific to the *Xoo* strain overexpressing Tal7b were identified (Figure 4), suggesting that effector Tal7b may target more than one gene in the rice genome. The use of computationally predicted EBE for Tal7b allowed for identification of gene candidates in or near each Tal7b-unique QTL (Figure 4b, c), and mapping of the EBE to promoter sequences for candidate genes mined for the MAGIC founder lines allowed detection of several types of promoter variations relative to the EBE (Figure 5). The promoter variants detected in at least one or more of the eight founder parents suggested that the resistance we detected in this study against Tal7b may be through a loss of susceptibility. Indeed, expanded phenotyping of AILs harbouring qBB-*tal7b*-8, a unique Tal7b QTL, revealed that AILs lacking the Tal7b target EBE in one gene target did not show enhanced susceptibility to Tal7b (Figure 5e). In contrast, AILs with the intact allele were more susceptible to *Xoo* with Tal7b. Thus, we suggest that the resistance mechanism governing qBB-*tal7b*-8 is through loss of susceptibility (Antony *et al.*, 2010; Huang *et al.*, 2016; Hutin *et al.*, 2015; Iyer and McCouch, 2004).

Overall, our study demonstrates that pathogen virulence factors that contribute quantitatively to disease can facilitate identification of effective minor disease resistance QTL for bacterial blight of rice. The indica MAGIC population, which captures the genetic diversity of eight parents (Bandillo *et al.*, 2013; Raghavan *et al.*, 2017), allowed for identification of novel QTL targeting Tal7b and for refinement of previously identified regions targeting *Xoo*. Because the parents of the indica MAGIC population are elite varieties, introgression of the identified resistance loci into commercial, farmer accepted varieties can be accelerated due to minimal linkage drag. While this study focuses on resistance to a bacterial disease of rice, the strategy for finding novel resistance based on knowledge of effector-targeted susceptibility and the application of the MAGIC genetic resources is broadly applicable to other crops and diseases.

Methods

Bacterial strains, inoculum preparation, plant material and growth conditions

The bacterial strains and plasmids used in this study are listed in Table S12 along with relevant characteristics. *Xoo* strains were cultured on Peptone Sucrose Agar (PSA) (Karganilla et al., 1973) at 28 °C and *Escherichia coli* strains were cultured on Luria–Bertani (LB) medium (Miller, 1992) at 37 °C. When necessary, antibiotics were added to the medium at the following concentrations: 50 µg/mL streptomycin, 50 µg/mL spectinomycin and 2 µg/mL tetracycline. To prepare inoculum, all strains were cultured for 24 h at 28 °C on PSA amended with streptomycin and spectinomycin. Bacteria were suspended in sterile water to 0.2 OD_{600}, approximately 10^8 CFU/mL.

Rice varieties used in this study include 330 AILs from the indica MAGIC population (Bandillo et al., 2013; Bossa-Castro et al., 2018; Raghavan et al., 2017) at the sixth to eighth generation of selfing (S6-S8), as well as the eight founding parents: Fedearroz 50, IR45427-2B-2-2b-1-1, IR4630-22-2-5-1-3, IR77298-14-1-2-10, PSBRc82, Samba Mashuri + Sub1, Sanhuangzhan-2 and PSBRc158. Nipponbare served as a susceptible control, respectively. Plants were grown and cared for as described (Bossa-Castro et al., 2018). Rice lines were grown in triplicate using an incomplete random block (IRB) design. For inoculations, the two youngest, completely expanded leaves of each six-week-old rice plant were leaf clip-inoculated with bacterial suspensions as described (Kauffman et al., 1973). Lesion lengths (LL) were measured in centimetres (cm) at 14 days postinoculation (dpi).

Lesion lengths were analysed using SAS® software version 9.4 (SAS Institute Inc., 2013). Each of the two inoculated leaves per plant was treated as technical replicates and used to calculate simple means for each biological replicate. All biological replicate values were then averaged using the least square means (LS-Means) function in PROC MIXED. Bacterial strain, line and bacterial strain by line interaction were treated as fixed effects. Block and replicates were treated as random effects. *P*-values were calculated using Tukey's method for multiple comparisons. AILs with missing phenotypic data were removed from all analyses.

Plasmid constructs

The *tal7b* gene, previously named *aB4.5* (Bai et al., 2000), was subcloned from a cosmid clone pXO6-33 derived from *Xoo* strain PXO86 (Hopkins et al., 1992), GenBank accession No. AJQ83546.1 (Booher et al., 2015), to generate pBS4.5b. The CRR of *tal7b* (*tal7b*) was cloned as an *Sph*I fragment into entry vector pCS466 to generate pCS466::*tal7b*. pCS466 is a derivative of the Gateway entry vector pCR8-GW (Invitrogen) that contains a truncated form of the *X. oryzae* pv. *oryzicola* BLS256 *tal1c* gene, from which the *Sph*I fragment that comprises the repeat region has been removed (Verdier et al., 2012). Using Gateway LR Clonase (Invitrogen), the *tal7b* CRR flanked by the *tal1c* N- and C-termini was transferred to the destination vector pKEB31 (Cermak et al., 2011), Addgene plasmid 31224 (www.addgene.org), to create pKEB31::*tal7b* for constitutive expression in *Xanthomonas*. Finally, *tal7b* was cloned into the low-copy cosmid vector pHM1 (Hopkins et al., 1992) by digesting pKEB31::*tal7b* with *Hind*III HF to extract the *tal7b* CRR flanked by the *tal1c* domains (Verdier et al., 2012). The resulting plasmid, pHM1::*tal7b* was transformed into *Xoo* PXO99^A by electroporation (Choi and Leach,

1994). Transformants were selected on nutrient agar containing appropriate antibiotics. Colony PCR with primers F4: CGCAATG-CACTGACGGGTGC and R2458: CATGCAAAGACGCCT-GATCCGG confirmed the presence of *tal7b* CRR. The PCR programme was 96 °C for 4 min, 25 repeats of 15 s at 96 °C, 30 s at 58 °C, 45 s at 70 °C and a final 70 °C for 4 min. Integrity of *tal7b* was confirmed by Sanger sequencing.

Genotyping

The 330 AILs and the eight founder parents used in this study were genotyped as part of a larger study conducted by the International Rice Research Institute. Sample preparation, genotyping by sequencing (GBS), data collection and analysis were carried out as described (Bandillo et al., 2013; Raghavan et al., 2017). Briefly, GBS libraries were generated using the 96-plex *ape*KI-based protocol according to (Elshire et al., 2011). Raw reads, publicly available at http://snpseek.irri.org/_download.zul, were trimmed and aligned to the Nipponbare reference genome MSUv7 (Kawahara et al., 2013). SNP calling was conducted prior to filtering as described in Raghavan et al. (2017). With a call rate of >70% and a minor allele frequency of >0.05, a total of 14,561 SNP markers remained to cover the rice genome. Approximate marker density was one SNP marker per 25.6 Kb (Figure S4). Overall SNP marker density allowed for genome wide association studies and QTL detection. SNP markers were named to indicate genomic location, that is the number following S is the chromosome number followed by the bp coordinate of the SNP in the MSU7 Nipponbare reference genome (Tables S6, S7).

Interval mapping

Interval mapping was carried out using the *mpIM* function from R package mpMap, a platform designed for QTL mapping of multi-parent populations (Huang and George, 2011). A linkage map was generated with the SNP data of each AIL and founder, as well as line pedigree. Interval mapping assumed true marker positions, no covariates and a step size of 1 cM. QTL position, founder effect estimate and allele effect were determined as described (Tables S4, S5; Bossa-Castro et al., 2018; Raghavan et al., 2017).

Genome-wide association studies

GWAS was performed as described (Bossa-Castro et al., 2018). Briefly, a kinship matrix was generated for the MAGIC population, excluding parents, to account for population structure using TASSEL version 5.0.2 (Bradbury et al., 2007). Statistics and allele effects were generated in TASSEL with the mixed linear model (MLM) function. Q-values, which assess the false discovery rate from GWAS, were calculated with q-value package in R (Storey and Tibshirani, 2003). The linear model settings were set to default, where compression level was calculated using the optimum level and the variance component estimated using the P3D method. Results are presented in Manhattan plots generated using the qqman R package (Turner, 2014).

Confirmation of resistance phenotype on chromosome 8

MAGIC AILs with the variant allele in the resistance locus on chromosome 8 (13, 24, 156, 163, 197, 210, 219, 222, 225, 229, 234, 237, 250, 267) were selected to confirm the resistance phenotype identified on chromosome 8. Nipponbare was used as a susceptible control. Six plants per AIL served as biological replicates and two leaves per plant served as technical replicates for each bacterial treatment. The two bacterial treatments were

PXO99[A] pHMI::EV or PXO99[A] pHMI::tal7b. At 14 dpi, lesion lengths were measured and data were analysed using one-way ANOVA. Statistical analyses were carried out using JMP Pro 13 (SAS Institute Inc., Cary, NC).

Physical map of QTL identified in this study, predicted Tal7b gene targets and known resistance genes/QTL

All reported BB resistance genes and QTL compiled in (Djedatin et al., 2016) were used to generate a physical map of the QTL identified in this study with respect to all known BB resistance loci. The maps were generated with tidyverse, a collection of R packages that include ggplot2 (Wickham, 2017). The physical position of resistance and susceptibility genes, QTL and predicted Tal7b gene targets were then superimposed onto each chromosome.

Tal7b-predicted targets

Tal7b gene targets were predicted using Talvez v3.1 and TALE-NT 2.0 (Doyle et al., 2012; Pérez-Quintero et al., 2015). Both programmes were run against the Nipponbare v. MSU7 rice reference genome (Kawahara et al., 2013). Predicted EBE were compared between both TAL prediction programmes, and, those that overlapped and were in close proximity to identified QTL were subjected to further analysis.

Gene expression data retrieval and analysis

Gene expression data used in this study were retrieved from the daTALbase http://bioinfo-web.mpl.ird.fr/cgi-bin2/datalbase/home.cgi (Pérez-Quintero et al., 2018).

Western blot analysis of Tal7b

Overnight liquid cultures of bacterial strains were pelleted and washed twice with deionized (DI) water. Bacterial pellets were resuspended in DI water and adjusted to an OD_{600} of 0.5. Cells were lysed, and protein was denatured with Laemmli buffer and heat. Total protein was separated on a 10% polyacrylamide gel followed by transfer to nitrocellulose. Tal7b was detected by TAL antibody (a gift from Adam Bogdanove, Cornell University), diluted 1:5000 and goat anti-rabbit HRP secondary antibody, diluted 1:2500.

Allelic variation in putative EBE sites and target gene promoter regions

Polymorphisms affecting putative Tal7b EBE sites of 113 target genes were examined in the region spanning the start codon to 1kb upstream of the EBE site. Variant Call Format (VCF) data from the rice 3K genomes project (Wang et al., 2018), based on an alignment to IR64 (reference genome for indica subgroup), were extracted from the genomes of the eight MAGIC parents (https://registry.opendata.aws/3kricegenome/). Using a python script, four types of mutations were identified and characterized; nucleotide substitutions within EBE site, insertions/deletions within the EBE site, insertions/deletions downstream or upstream of EBE site or complete deletion of EBE and/or surrounding promoter region (Table S9). Consensus sequences for each region were generated using the VCF data and were aligned using Clustal Omega for visualization (https://www.ebi.ac.uk/).

Conflict of interest

The authors declare no conflict of interest.

Author contributions

A.I.H., E.E.D., A.M.B.-C., H.L., V.V. and J.E.L. designed research; A.I.H., E.E.D., A.M.B.-C., B.W.T., R.C., A.P.-Q and V.V. performed research; A.I.H., E.E.D., A.M.B.-C. and J.E.L. analysed data; A.I.H., E.E.D. and J.E.L. wrote the paper.

References

Antony, G., Zhou, J., Huang, S., Li, T., Liu, B., White, F. and Yang, B. (2010) Rice xa13 recessive resistance to bacterial blight is defeated by induction of the disease susceptibility gene Os-11N3. Plant Cell 22, 3864–3876.

Ashkani, S., Rafii, M., Rahim, H. and Latif, M. (2013) Mapping of the quantitative trait locus (QTL) conferring partial resistance to rice leaf blast disease. Biotechnol. Lett. 35, 799–810.

Bai, J., Choi, S.-H., Ponciano, G., Leung, H. and Leach, J.E. (2000) Xanthomonas oryzae pv. oryzae avirulence genes contribute differently and specifically to pathogen aggressiveness. Mol. Plant Microbe Interact. 13, 1322–1329.

Bandillo, N., Raghavan, C., Muyco, P.A., Sevilla, M.A.L., Lobina, I.T., Dilla-Ermita, C.J., Tung, C.-W. et al. (2013) Multi-parent advanced generation inter-cross (MAGIC) populations in rice: progress and potential for genetics research and breeding. Rice 6, 11.

Blair, M.W., Garris, A.J., Iyer, A.S., Chapman, B., Kresovich, S. and McCouch, S.R. (2003) High resolution genetic mapping and candidate gene identification at the xa5 locus for bacterial blight resistance in rice (Oryza sativa L.). Theor. Appl. Genet. 107, 62–73.

Boch, J., Scholze, H., Schornack, S., Landgraf, A., Hahn, S., Kay, S., Lahaye, T. et al. (2009) Breaking the code of DNA binding specificity of TAL-type III effectors. Science 326, 1509–1512.

Boch, J., Bonas, U. and Lahaye, T. (2014) TAL effectors–pathogen strategies and plant resistance engineering. New Phytol. 204, 823–832.

Booher, N.J., Carpenter, S.C., Sebra, R.P., Wang, L., Salzberg, S.L., Leach, J.E. and Bogdanove, A.J. (2015) Single molecule real-time sequencing of Xanthomonas oryzae genomes reveals a dynamic structure and complex TAL (transcription activator-like) effector gene relationships. Microb. Genom. 1. https://doi.org/10.1099/mgen.0.000032

Bossa-Castro, A.M., Tekete, C., Raghavan, C., Delorean, E.E., Dereeper, A., Dagno, K., Koita, O. et al. (2018) Allelic variation for broad-spectrum resistance and susceptibility to bacterial pathogens identified in a rice MAGIC population. Plant Biotechnol J. 16, 1559–1568.

Bradbury, P.J., Zhang, Z., Kroon, D.E., Casstevens, T.M., Ramdoss, Y. and Buckler, E.S. (2007) TASSEL: software for association mapping of complex traits in diverse samples. Bioinformatics 23, 2633–2635.

Cermak, T., Doyle, E.L., Christian, M., Wang, L., Zhang, Y., Schmidt, C., Baller, J.A., Somia, N.V., Bogdanove, A.J. and Voytas, D.F. (2011) Efficient design and assembly of custom TALEN and other TAL effector-based constructs for DNA targeting. Nucleic Acids Res., 39(12), e82. https://doi.org/10.1093/nar/gkr218

Chen, L.N., Yang, Y., Yan, C.Q., Wang, X.M., Yu, C.L., Zhou, J., Zhang, W.L. *et al.* (2012) Identification of quantitative trait loci for bacterial blight resistance derived from *Oryza meyeriana* and agronomic traits in recombinant inbred lines of *Oryza sativa*. *Int. J. Phytopathol.* **160**, 461–468.

Choi, S.H. and Leach, J.E. (1994) Genetic manipulation of *Xanthomonas oryzae* pv. *oryzae*. *Int. Rice Res. Notes* **19**, 31–32.

Cohn, M., Bart, R.S., Shybut, M., Dahlbeck, D., Gomez, M., Morbitzer, R., Hou, B.-H. *et al* (2014) *Xanthomonas axonopodis* virulence is promoted by a transcription activator-like effector–mediated induction of a *SWEET* sugar transporter in cassava. *Mol. Plant Microbe Interact.* **27**, 1186–1198.

Cox, K.L., Meng, F., Wilkins, K.E., Li, F., Wang, P., Booher, N.J., Carpenter, S.C.D. *et al*. (2017) TAL effector driven induction of a *SWEET* gene confers susceptibility to bacterial blight of cotton. *Nat. Commun.* **8**, 15588.

Djedatin, G., Ndjiondjop, M.-N., Sanni, A., Lorieux, M., Verdier, V. and Ghesquiere, A. (2016) Identification of novel major and minor QTLs associated with *Xanthomonas oryzae* pv. *oryzae* (African strains) resistance in rice (*Oryza sativa* L.). *Rice* **9**, 18.

Doyle, E.L., Booher, N.J., Standage, D.S., Voytas, D.F., Brendel, V.P., VanDyk, J.K. and Bogdanove, A.J. (2012) TAL Effector-Nucleotide Targeter (TALE-NT) 2.0: tools for TAL effector design and target prediction. *Nucleic Acids Res.* **40**, W117–W122.

Elshire, R.J., Glaubitz, J.C., Sun, Q., Poland, J.A., Kawamoto, K., Buckler, E.S. and Mitchell, S.E. (2011) A robust, simple genotyping-by-sequencing (GBS) approach for high diversity species. *PLoS One* **6**, e19379.

Hopkins, C.M., White, F.F., Choi, S.H., Guo, A. and Leach, J.E. (1992) Identification of a family of avirulence genes from *Xanthomonas oryzae* pv. *oryzae*. *Mol. Plant Microbe Interact.* **5**, 451–459.

Huang, B.E. and George, A.W. (2011) R/mpMap: a computational platform for the genetic analysis of multiparent recombinant inbred lines. *Bioinformatics* **27**, 727–729.

Huang, S., Antony, G., Li, T., Liu, B., Obasa, K., Yang, B. and White, F.F. (2016) The broadly effective recessive resistance gene *xa5* of rice is a virulence effector-dependent quantitative trait for bacterial blight. *Plant J.* **86**, 186–194.

Hutin, M., Pérez-Quintero, A.L., Lopez, C. and Szurek, B. (2015) MorTAL Kombat: the story of defense against TAL effectors through loss-of-susceptibility. *Front. Plant Sci.* **6**, 535.

Iyer, A.S. and McCouch, S.R. (2004) The rice bacterial blight resistance gene *xa5* encodes a novel form of disease resistance. *Mol. Plant Microbe Interact.* **17**, 1348–1354.

Karganilla, A., Natural, M. and Ou, S. (1973) A comparative study of culture media for *Xanthomonas oryzae* [bacterial leaf blight of rice]. *Philipp Agric.* **57**, 141–152.

Kauffman, H., Reddy, A., Hsiek, S. and Merca, S. (1973) An improved technique for evaluating resistance of rice varieties to *Xanthomonas oryzae*. *Plant Dis. Rep.* **57**, 537–541.

Kawahara, Y., de la Bastide, M., Hamilton, J.P., Kanamori, H., McCombie, W.R., Ouyang, S., Schwartz, D.C. *et al*. (2013) Improvement of the *Oryza sativa* Nipponbare reference genome using next generation sequence and optical map data. *Rice* **6**, 4.

Lang, J.M., Pérez-Quintero, A.L., Koebnik, R., DuCharme, E., Sarra, S., Doucoure, H., Keita, I. *et al*. (2019) A pathovar of *Xanthomonas oryzae* infecting wild grasses provides insight into the evolution of pathogenicity in rice agroecosystems. *Front. Plant Sci.* **10**, 507.

Leach, J.E., Vera-Cruz, C.M., Bai, J. and Leung, H. (2001) Pathogen fitness penalty as a predictor of durability of disease resistance genes. *Annu. Rev. Phytopathol.* **39**, 187–224.

Mew, T.W., Vera, C. and Medalla, E.S. (1992) Changes in race frequency of *Xanthomonas oryzae* pv. *oryzae* in response to rice cultivars planted in the Philippines. *Plant Dis.* **76**, 1029.

Miller, J.H. (1992) *A Short Course in Bacterial Genetics: A Laboratory Manual and Handbook for Escherichia coli and Related Bacteria*. Cold Spring Harbor, NY: Cold Spring Harbor Laboratory Press.

Moscou, M.J. and Bogdanove, A.J. (2009) A simple cipher governs DNA recognition by TAL effectors. *Science* **326**, 1501.

Mundt, C.C. (2014) Durable resistance: a key to sustainable management of pathogens and pests. *Infect. Genet. Evol.* **27**, 446–455.

Oliva, R., Ji, C., Atienza-Grande, G., Huguet-Tapia, J.C., Perez-Quintero, A., Li, T., Eom, J.-S. *et al*. (2019) Broad-spectrum resistance to bacterial blight in rice using genome editing. *Nat. Biotechnol.* **37**, 1344–1350.

Pérez-Quintero, A.L., Rodriguez-R, L.M., Dereeper, A., López, C., Koebnik, R., Szurek, B. and Cunnac, S. (2013) An improved method for TAL effectors DNA-binding sites prediction reveals functional convergence in TAL repertoires of *Xanthomonas oryzae* strains. *PLoS One* **8**, e68464.

Pérez-Quintero, A.L., Lamy, L., Gordon, J., Escalon, A., Cunnac, S., Szurek, B. and Gagnevin, L. (2015) QueTAL: a suite of tools to classify and compare TAL effectors functionally and phylogenetically. *Front. Plant Sci.* **6**, 545.

Pérez-Quintero, A.L., Lamy, L., Zarate, C.A., Cunnac, S., Doyle, E., Bogdanove, A., Szurek, B. *et al*. (2018) daTALbase: A database for genomic and transcriptomic data related to TAL effectors. *Mol. Plant Microbe. Interact.* **31**, 471–480.

Perez-Quintero, A.L. and Szurek, B. (2019) A decade decoded: Spies and hackers in the history of TAL effectors research. *Annu Rev. Phytopathol.* **57**, 459–481.

Ponciano, G., Ishihara, H., Tsuyumu, S. and Leach, J.E. (2003) Bacterial effectors in plant disease and defense: keys to durable resistance? *Plant Dis.* **87**, 1272–1282.

Quibod, I.L., Perez-Quintero, A., Booher, N.J., Dossa, G.S., Grande, G., Szurek, B., Vera Cruz, C. *et al*. (2016) Effector diversification contributes to *Xanthomonas oryzae* pv. *oryzae* phenotypic adaptation in a semi-isolated environment. *Sci. Rep.* **6**, 34137.

Raghavan, C., Mauleon, R., Lacorte, V., Jubay, M., Zaw, H., Bonifacio, J., Singh, R.K. *et al*. (2017) Approaches in characterizing genetic structure and mapping in a rice multiparental population. *G3* **7**, 1721–1730.

Römer, P., Recht, S., Strauß, T., Elsaesser, J., Schornack, S., Boch, J., Wang, S. *et al*. (2010) Promoter elements of rice susceptibility genes are bound and activated by specific TAL effectors from the bacterial blight pathogen, *Xanthomonas oryzae* pv. oryzae . *New Phytol.* **187**, 1048–1057.

Schornack, S., Ballvora, A., Gürlebeck, D., Peart, J., Ganal, M., Baker, B., Bonas, U. *et al*. (2004) The tomato resistance protein Bs4 is a predicted non-nuclear TIR-NB-LRR protein that mediates defense responses to severely truncated derivatives of AvrBs4 and overexpressed AvrBs3. *Plant J.* **37**, 46–60.

Storey, J.D. and Tibshirani, R. (2003) Statistical significance for genomewide studies. *Proc. Natl. Acad. Sci. USA* **100**, 9440–9445.

Streubel, J., Pesce, C., Hutin, M., Koebnik, R., Boch, J. and Szurek, B. (2013) Five phylogenetically close rice *SWEET* genes confer TAL effector-mediated susceptibility to *Xanthomonas oryzae* pv. *oryzae*. *New Phytol.* **200**, 808–819.

Tello-Ruiz, M.K., Naithani, S., Stein, J.C., Gupta, P., Campbell, M., Olson, A., Wei, S. *et al*. (2017) Gramene 2018: unifying comparative genomics and pathway resources for plant research. *Nucleic Acids Res.* **46**, D1181–D1189.

Triplett, L.R., Cohen, S.P., Heffelfinger, C., Schmidt, C.L., Huerta, A.I., Tekete, C., Verdier, V. *et al*. (2016) A resistance locus in the American heirloom rice variety Carolina Gold Select is triggered by TAL effectors with diverse predicted targets and is effective against African strains of *Xanthomonas oryzae* pv. *oryzicola*. *Plant J.* **87**, 472–483.

Turner, S.D. (2014) qqman: an R package for visualizing GWAS results using QQ and manhattan plots.. *BioRxiv*. https://doi.org/10.1101/005165

Vera Cruz, C., Bai, J., Oña, I., Leung, H., Nelson, R., Mew, T. and Leach, J.E. (2000) Predicting durability of a disease resistance gene based on an assessment of the fitness loss and epidemiological consequences of avirulence gene mutation. *Proc. Natl. Acad. Sci. USA* **97**, 13500–13505.

Verdier, V., Triplett, L.R., Hummel, A.W., Corral, R., Cernadas, R.A., Schmidt, C.L., Bogdanove, A.J. *et al*. (2012) Transcription activator-like (TAL) effectors targeting OsSWEET genes enhance virulence on diverse rice (*Oryza sativa*) varieties when expressed individually in a TAL effector-deficient strain of *Xanthomonas oryzae*. *New Phytol.* **196**, 1197–1207.

Wang, W., Mauleon, R., Hu, Z., Chebotarov, D., Tai, S., Wu, Z., Li, M. *et al*. (2018) Genomic variation in 3,010 diverse accessions of Asian cultivated rice. *Nature* **557**, 43–49.

Wickham, H. (2017) *Tidyverse: Easily install and load'Tidyverse'Packages: R package version 1.1. 0*.

Yang, B. and White, F.F. (2004) Diverse members of the AvrBs3/PthA family of type III effectors are major virulence determinants in bacterial blight disease of rice. *Mol. Plant Microbe Interact.* **17**, 1192–1200.

Yang, B., Zhu, W., Johnson, L.B. and White, F.F. (2000) The virulence factor AvrXa7 of *Xanthomonas oryzae* pv. *oryzae* is a type III secretion pathway-dependent nuclear-localized double-stranded DNA-binding protein. *Proc. Natl. Acad. Sci. USA* **97**, 9807–9812.

Yang, B., Sugio, A. and White, F.F. (2006) *Os8N3* is a host disease-susceptibility gene for bacterial blight of rice. *Proc. Natl. Acad. Sci. USA* **103**, 10503–10508.

Zhang, J., Yin, Z. and White, F. (2015) TAL effectors and the executor R genes. *Front. Plant Sci.* **6**, 641.

Supporting information

Additional supporting information may be found online in the Supporting Information section at the end of the article.

Figure S1 Amino acid identity matrix for the 15 Tal7b homologues in geographically distinct Asian strains of X. o. pv. oryzae.

Figure S2 Western blot confirming overexpression of Tal7b in PXO99[A] (pHMI::*tal7b*). WT = PXO99[A]. The product of the *tal7b* gene, marked with arrow, is 124 kDa.

Figure S3 Interval mapping shows QTL detected to *Xoo* (a) PXO99[A] pHM1::EV and (b) PXO99[A] pHM1::*tal7b* in the indica MAGIC population.

Figure S4 SNP Marker Density.

Table S1 Indica MAGIC population response to PXO99[A] pHM1::EV and pHMI::*tal7b*.

Table S2 Mixed model ANOVA for the indica MAGIC population screened in response to PXO99[A] pHMI::EV and PXO99[A] pHMI::*tal7b*.

Table S3 Response of indica MAGIC parents to PXO99[A] pHM1::EV and PXO99[A] pHM1::*tal7b*.

Table S4 QTL detected in indica MAGIC population to *Xoo*PXO99[A] pHM1::EV.

Table S5 QTL detected in indica MAGIC population to *Xoo*PXO99[A] pHM1::*tal7b*.

Table S6 Significant SNPs associated with disease resistance to *Xoo*PXO99[A] pHM1::EV in indica MAGIC population.

Table S7 Significant SNPs associated with disease resistance to *Xoo*PXO99[A] pHM1::*tal7b* in indica MAGIC population.

Table S8 Resistance QTL identified to PXO99[A] pHMI::EV and PXO99[A] pHMI::*tal7b* and putative Tal7b gene targets in reference to previously described resistance loci for bacterial blight in rice.

Table S9 Gene induction of putative Tal7b gene targets in Nipponbare and IR24, two susceptible rice verities to *X. o.* pv. *oryzae,* and genomic variation in the EBE and coding sequence of the same genes in the eight MAGIC founders

Table S10 Phenotypic response of 14 indica MAGIC advanced inbred lines (AIL) with variant allele in qBB-*tal7b*-8 on chromosome 8 to PXO99[A] pHMI::*tal7b*.

Table S11 Bacterial strains and plasmids used in this study.